NEOPLASIA
www.neoplasia.com

Volume 13 Number 6 June 2011 pp. 526–536 526

Androgen Depletion Induces Senescence in Prostate Cancer Cells through Down-regulation of Skp2[1,2]

Zuzana Pernicová*, Eva Slabáková*, Gvantsa Kharaishvili†, Jan Bouchal†, Milan Král‡, Zuzana Kunická§, Miroslav Machala¶, Alois Kozubík*,§ and Karel Souček*

*Department of Cytokinetics, Institute of Biophysics, AS CR, Brno, Czech Republic; †Laboratory of Molecular Pathology and Institute of Molecular and Translational Medicine, Faculty of Medicine and Dentistry, Palacky University, Olomouc, Czech Republic; ‡Department of Urology, University Hospital, Olomouc, Czech Republic; §Department of Experimental Biology, Faculty of Science, Masaryk University, Brno, Czech Republic; ¶Department of Chemistry and Toxicology, Veterinary Research Institute, Brno, Czech Republic

Abstract

Although the induction of senescence in cancer cells is a potent mechanism of tumor suppression, senescent cells remain metabolically active and may secrete a broad spectrum of factors that promote tumorigenicity in neighboring malignant cells. Here we show that androgen deprivation therapy (ADT), a widely used treatment for advanced prostate cancer, induces a senescence-associated secretory phenotype in prostate cancer epithelial cells, indicated by increases in senescence-associated β-galactosidase activity, heterochromatin protein 1β foci, and expression of cathepsin B and insulin-like growth factor binding protein 3. Interestingly, ADT also induced high levels of vimentin expression in prostate cancer cell lines *in vitro* and in human prostate tumors *in vivo*. The induction of the senescence-associated secretory phenotype by androgen depletion was mediated, at least in part, by down-regulation of S-phase kinase-associated protein 2, whereas the neuroendocrine differentiation of prostate cancer cells was under separate control. These data demonstrate a previously unrecognized link between inhibition of androgen receptor signaling, down-regulation of S-phase kinase-associated protein 2, and the appearance of secretory, tumor-promoting senescent cells in prostate tumors. We propose that ADT may contribute to the development of androgen-independent prostate cancer through modulation of the tissue microenvironment by senescent cells.

Neoplasia (2011) 13, 526–536

Abbreviations: ADT, androgen deprivation therapy; AIPC, androgen-independent prostate cancer; AR, androgen receptor; CS, charcoal-stripped fetal bovine serum; EMT, epithelial-to-mesenchymal transition; HP1β, heterochromatin protein 1β; IL-8, interleukin-8; IGFBP3, insulin-like growth factor binding protein 3; NED, neuroendocrine differentiation; SA-β-gal, senescence-associated β-galactosidase; SASP, senescence-associated secretory phenotype; Skp2, S-phase kinase-associated protein 2

Address all correspondence to: Karel Souček, PhD, Institute of Biophysics, AS CR, Královopolská 135, CZ-612 65 Brno, Czech Republic. E-mail: ksoucek@ibp.cz

[1]This work was supported by grants IGA MZD 9600-4/2008 and 9956-3/2008, and by a grant from the Czech Science Foundation 310/07/0961. Institutional support comes from grant nos. AV0Z50040507 and AV0Z50040702 from the Academy of Sciences of the Czech Republic, grant nos. MSM0021622430 and MSM6198959216 from the Ministry of Education, Youth and Sports of the Czech Republic, and EU infrastructure support CZ.1.05/2.1.00/01.0030. The authors declare no conflict of interest.
[2]This article refers to supplementary materials, which are designated by Table W1 and Figures W1 to W3 and are available online at www.neoplasia.com.
Received 19 January 2011; Revised 9 March 2011; Accepted 10 March 2011

DOI 10.1593/neo.11182

Introduction

Androgen deprivation therapy (ADT) is an important treatment for advanced stage prostate cancer and is achieved by androgen receptor (AR) blockade and/or medical or surgical castration [1,2]. Although ADT is initially very effective, treated tumors inevitably progress to androgen-independent prostate cancer (AIPC), which is currently incurable and fatal. The mechanism through which ADT causes androgen independence is therefore of considerable clinical importance.

One possible mechanism for the development of AIPC is modulation of the tissue microenvironment by neuroendocrine (NE)-like cancer cells, which emerge after ADT [3,4]. NE-like cancer cells are capable of regulating the proliferation, invasion, and secretory activity of surrounding cells through a paracrine mechanism involving a range of secreted neuropeptides and cytokines (e.g., gastrin-releasing peptide, serotonin, interleukin-8 (IL-8) [5]). The impact of the microenvironment on prostate cancer progression may be further enhanced by tumor heterogeneity characterized by the presence of multiple foci of proliferative inflammatory atrophy, high-grade prostatic intraepithelial neoplasia, and carcinoma in the peripheral zone of prostate [6].

Activation of AR signaling by a variety of growth factors and cytokines, such as insulin-like growth factor 1, keratinocyte growth factor, epidermal growth factor [7], IL-6 [8], or IL-8 [9], may also contribute to development of AIPC [10]. Significantly, these factors may also be secreted by senescent epithelial cells [11]. Senescence is a general cell biologic phenomenon that limits the life span of cells and prevents unlimited cell proliferation. Although senescent cells do not proliferate, they are resistant to apoptosis and remain metabolically active [12]. Irreversible cell cycle arrest, the hallmark of senescence, can be triggered by a variety of stimuli including deregulated expression of some oncogenes [13,14] or tumor suppressors [15,16], telomere shortening [17], oxidative stress [18], and chemotherapeutic drugs [19,20]. For these reasons, induction of senescence is a potent defense against tumorigenesis. There is a dark side to this defense mechanism, however: metabolically active senescent cells may promote tumorigenicity of neighboring malignant cells through the secretion of a range of growth factors and cytokines [11,21,22]. Aged fibroblasts with this senescence-associated secretory phenotype (SASP) are not the only cells capable of modulating the prostate microenvironment and promoting carcinogenesis [23]; senescent prostate epithelial cells can also behave in this manner [24].

Senescence can be induced by a variety of signaling pathways, such as p53-p21$^{Cip1/Waf}$, p19^{Arf}-p53, and p16^{INK4a}-RB [25], which may interact with one another or act independently to arrest cell proliferation [12]. Recently, S-phase kinase-associated protein 2 (Skp2) was shown to play an important role in the promotion of senescence by oncogenic Ras or by inactivation of PTEN [26]. Skp2, a crucial component of the Skp, Cullin, F-box–containing complex, is an E3 ligase involved in cell cycle progression through degradation of p27^{Kip1} and other targets [27]. Elevation of Skp2 occurs in a variety of cancers, including prostate [28,29]. Interestingly, Skp2 is regulated by AR signaling, and inhibition of AR leads to down-regulation of Skp2 and decreased cell proliferation [30,31].

Here we show that ADT induces senescence and neuroendocrine differentiation (NED) of prostate cancer cells. Our results reveal a previously unsuspected relationship between the inhibition of AR signaling, down-regulation of Skp2, and the appearance of highly metabolically active tumor-promoting senescent cells in prostate cancer tissue. We propose that this mechanism plays a significant contribution to prostate tumor progression.

Materials and Methods

Cell Cultures and Androgen Depletion

LNCaP cells (human prostate carcinoma cells; DSMZ, Braunschweig, Germany) were cultivated in phenol red–free RPMI 1640 media (Invitrogen, Carlsbad, CA) supplemented with $NaHCO_3$ (Sigma Aldrich, St Louis, MO), penicillin/streptomycin, and 5% fetal bovine serum (FBS; both PAA, Pasching, Austria). For androgen depletion studies, LNCaP cells were cultivated in 5% dextran/charcoal-stripped FBS (CS). LAPC-4 cells (xenograft-derived human prostate carcinoma cells [32]) were cultivated in Iscove modified Dulbecco medium (Invitrogen) supplemented with $NaHCO_3$, penicillin/streptomycin, 10% FBS, and 1 nM R1881 (PerkinElmer, Waltham, MA). For androgen depletion studies, cells were cultivated in Iscove modified Dulbecco medium with 10% CS. All cells were grown in a humidified incubator (37°C, 5% CO_2).

Androgen-Depleted Cell Growth Conditions

For the induction of senescence and NED, the cells were seeded in appropriate growth medium with FBS, grown for 24 hours, and at day 0, the growth medium was replaced with growth medium supplemented with either complete FBS or CS. Cells were cultivated without reseeding for 2 to 16 days, medium was changed twice a week, and cells were harvested on days 2, 4, 8, and 16.

Western Blot Analysis of Cell Extracts

Protein extract preparation, gel electrophoresis, and Western blot analysis were performed as previously described [33] using antibodies described in Supplementary Materials and Methods. α-Tubulin or β-actin was used as loading controls. Signal densities were analyzed using ImageJ software (National Institutes of Health, Bethesda, MD) and normalized to the appropriate loading control.

Detection of Telomerase Activity

Telomerase activity was detected using TRAPeze XL Telomerase Detection Kit (Millipore, Billerica, MA) according to the manufacturer's recommendation.

Immunofluorescence and Confocal Microscopy

Cells were fixed and stained with appropriate antibodies as described in Supplementary Materials and Methods, and nuclei were visualized by counterstaining with TOPRO-3 (Invitrogen) or DAPI (4′, 6-diamidino-2-phenylindole; AppliChem, Darmstadt, Germany). Fluorescent-stained samples were mounted in Mowiol 4-88/DABCO (Calbiochem, Merck, Darmstadt, Germany) and viewed on a LSM Leica SP5 (Leica Microsystems, Wetzlar, Germany) confocal microscope.

Flow Cytometry and Detection of Intracellular Antigens

Trypsinized cells were fixed in 2% paraformaldehyde at 4°C, permeabilized, and incubated with appropriate antibodies (described in Supplementary Materials and Methods) diluted in PBS with 300 μg/ml digitonin. Stained cells were analyzed on a FACSCalibur or FACS Aria II Sorp (Becton Dickinson, San Jose, CA) cell sorter, and flow cytometry data were analyzed using FlowJo software (TreeStar, Ashland, OR). The median fluorescence index (MFI) was calculated as the ratio of

the median of fluorescence of the specific antibody and the median of fluorescence of the isotype control.

Senescence-Associated β-Galactosidase Analysis

Senescence-associated β-galactosidase (SA-β-gal) cytochemistry was performed at pH 6.0 using X-gal substrate (5-bromo-4-chloro-3-indolyl-β-D-galactopyranoside; Pierce, Rockford, IL) as previously described [34] and photographed using an Olympus IX-71 microscope (Olympus Europe, Hamburg, Germany). SA-β-gal activity was quantified using the fluorescent substrate 4-methylumbelliferyl-β-D-galactopyranoside (AppliChem) as described previously [35], with minor modifications. Fluorescence intensity was measured using a BMG FLUOStar Galaxy (BMG LABTECH, Offenburg, Germany) plate reader and normalized to the mean fluorescence intensity of the cells grown for 2 days in FBS.

Detection of Cathepsin B by Enzyme-Linked Immunosorbent Assay

Cathepsin B levels in medium conditioned by either LNCaP or LAPC-4 cells (see Supplementary Materials and Methods) were quantified using the human Cathepsin B DuoSet Enzyme-Linked Immunosorbent Assay (ELISA) Kit (DY2176; R&D Systems, Minneapolis, MN), according to the manufacturer's recommendations.

Cell Transfection and RNA Interference

DNA transfections were performed using Xfect transfection reagent (Clontech, Mountain View, CA). Briefly, cells were exposed to 5 μg of Skp2 mammalian expression vector (a kind gift from Keiichi I. Nakayama, Kyushu University, Japan) in antibiotic-free Dulbecco modified Eagle medium (DMEM) supplemented with 10% FBS for 4 hours, followed by 72 hours in DMEM supplemented with either FBS or CS. For RNA interference studies, cells were incubated for 4 hours in Opti-MEM medium (Invitrogen), followed by transfection with 10- to 40-nM small interfering RNA (siRNA) duplexes (Santa Cruz Biotechnology, Santa Cruz, CA) directed against PTEN (sc-44272), Skp2 (sc-36499), or nontargeted control (sc-37007) using X-treme transfection reagent (Roche, Bazel, Switzerland), according to the manufacturer's recommendations. Cells were harvested 48 hours after transfection.

Immunostaining of Human Prostate Cancer Cells

Formalin-fixed, paraffin-embedded human prostate tumor samples were obtained from an archive collected between 1998 and 2003 (Table W1). Samples were either fine-needle biopsies (preneoadjuvant ADT) or prostatectomies (postneoadjuvant ADT), and all patients were without distant metastases. Untreated control tumors (fine needle biopsies) were randomly selected. Samples were immunostained with appropriate antibodies (described in Supplementary Materials and Methods) using routine methods. Specimens were assessed semiquantitatively by histoscore (percentage of positivity in the area of interest multiplied by staining intensity categorized as follows: 0, absent; 1, weak; 2, moderate; and 3, strong).

Statistical Analysis

Statistical analysis was performed using STATISTICA for Windows (StatSoft, Prague, Czech Republic) using one-way analysis of variance followed by the Tukey range test. If the data variances were nonhomogeneous, Kruskal-Wallis one-way analysis was performed.

Results

Long-term Androgen Depletion Induces Senescence in Prostate Cancer Cells

Long-term androgen depletion induces cell cycle arrest without apoptosis in LNCaP and LAPC-4 prostate cancer cells (data not shown). In many cell types, irreversible cell cycle arrest correlates with senescence. We used senescence-associated β-galactosidase (SA-β-gal) activity, a general marker of senescence, to examine whether LNCaP and LAPC-4 cells became senescent after androgen depletion; hydrogen peroxide–treated human foreskin fibroblast (HFF-1) cells were used as a positive control (Figure W1*A*). Using a cytochemical reaction, many LNCaP cells were strongly positive for SA-β-gal after 16 days growth without androgens (Figure 1*A*). Quantification of SA-β-gal reactivity using a fluorescent substrate showed that androgen depletion led to a statistically significant increase in SA-β-gal activity in both LNCaP and LAPC-4 cells compared with control cells cultivated in the presence of androgens (Figure 1*B*). We observed differences in the kinetics of senescence induction in LNCaP and LAPC-4 cells. These differences were in correlation with the sensitivity of a particular cell line to the androgen deprivation and cell cycle arrest induction (data not shown). LNCaP cells were more sensitive to androgen deprivation in terms of inhibition of proliferation and showed a significant increase in SA-β-gal level at day 4 of cultivation in CS; however, more tumorigenic LAPC-4 cells were more resistant to the cell cycle arrest induction in the androgen-deprived condition and showed a significant increase in SA-β-gal level at day 8 of cultivation in CS.

To firmly establish the senescent phenotype of prostate cancer cells after ADT, we examined nuclear markers of senescence. Using TRAP (telomere repeat amplification protocol) to assay the telomerase activity, which is downregulated in senescent cells [36], we found that telomerase activity was almost undetectable in LNCaP cells after 8 days of cultivation without androgens relative to control cells grown in complete FBS (Figure 1*C*). Using immunostaining, we examined two chromatin markers of senescence: phosphorylated histone H2AX (S139) and heterochromatin protein 1β (HP1β), a component of heterochromatin foci, which were both significantly increased in senescent HFF-1 (Figure W1*B*). Both HP1β-positive heterochromatin foci and phospho-H2AX staining were increased by growth in androgen-depleted media, consistent with these cells becoming senescent (Figure 1*D*). Although phospho-H2AX staining was also increased by cultivation for 16 days in the presence of androgens, the effect of androgen depletion was evident as early as day 2. Taken together, these data indicate that androgen depletion induced senescence in cultured prostate cancer cell lines.

Androgen Depletion Induces a SASP in Prostate Cancer Cells

Recent findings have shown that senescent tumor cells are capable of promoting tumorigenesis through their secretion of growth factors and cytokines that have paracrine effects on nonsenescent neighboring cells [11]. We looked for evidence of this SASP in our *in vitro* model system by analyzing the expression of two components of the senescence secretome [11]: insulin-like growth factor-binding protein 3 (IGFBP3) and cathepsin B. Using flow cytometry, we found that IGFBP3 was significantly upregulated in prostate cancer cells cultivated for 8 days without androgens (Figure 2*A*). Using ELISA to analyze the cell-conditioned medium, we found that cathepsin B secretion from cells cultivated without androgens for 8 days was increased by more than 100% relative to control cells (Figure 2*B*). NED, a frequent

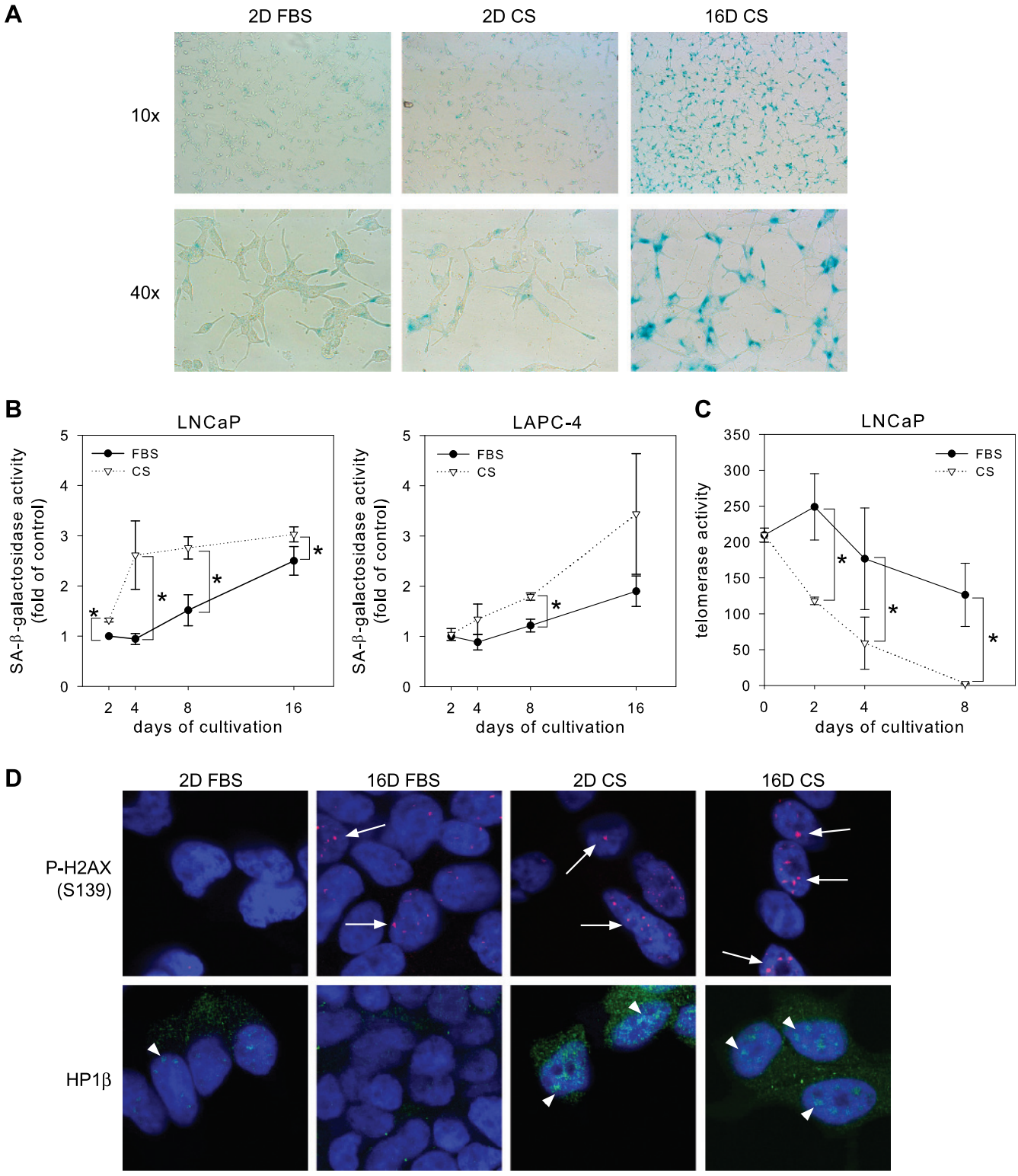

Figure 1. Androgen depletion induces senescence in prostate cancer cells. (A) Cytochemical detection of SA-β-gal activity in LNCaP cells cultivated in presence (FBS) or absence (CS) of androgens for 2 or 16 days (2D, 16D). (B) Quantitative analysis of SA-β-gal activity in LNCaP and LAPC-4 cells using fluorescent substrate. *Statistically significant changes ($P < .05$) compared with FBS-treated cells. (C) TRAP assay to detect telomerase activity in LNCaP cells. (D) Immunofluorescent detection of HP1β and P-H2AX (S139) in LNCaP cells. White arrows and arrowheads indicate P-H2AX (S139) staining and HP1β-positive foci, respectively.

finding after ADT of human prostate cancer patients [4], was also observed in our *in vitro* model system, based on increased levels of the widely used NED markers γ-enolase and tubulin β-III (data not shown). To determine whether functional NE-like cells were present in our cultures, we used flow cytometry to analyze intracellular levels of serotonin and histamine. Cells cultivated for 8 days under androgen-depleted conditions expressed higher intracellular levels of both these NE markers compared with cells cultivated in the presence of androgens (Figure 2, *C* and *D*).

We next examined the reversibility of cell cycle arrest induced by androgen depletion (Figure W2). After cultivating for 16 days in medium with (FBS) or without (CS) androgens, LNCaP cells were reseeded at a low density in the appropriate medium. When cells were cultivated in FBS and reseeded in FBS, SA-β-gal reactivity was substantially reduced.

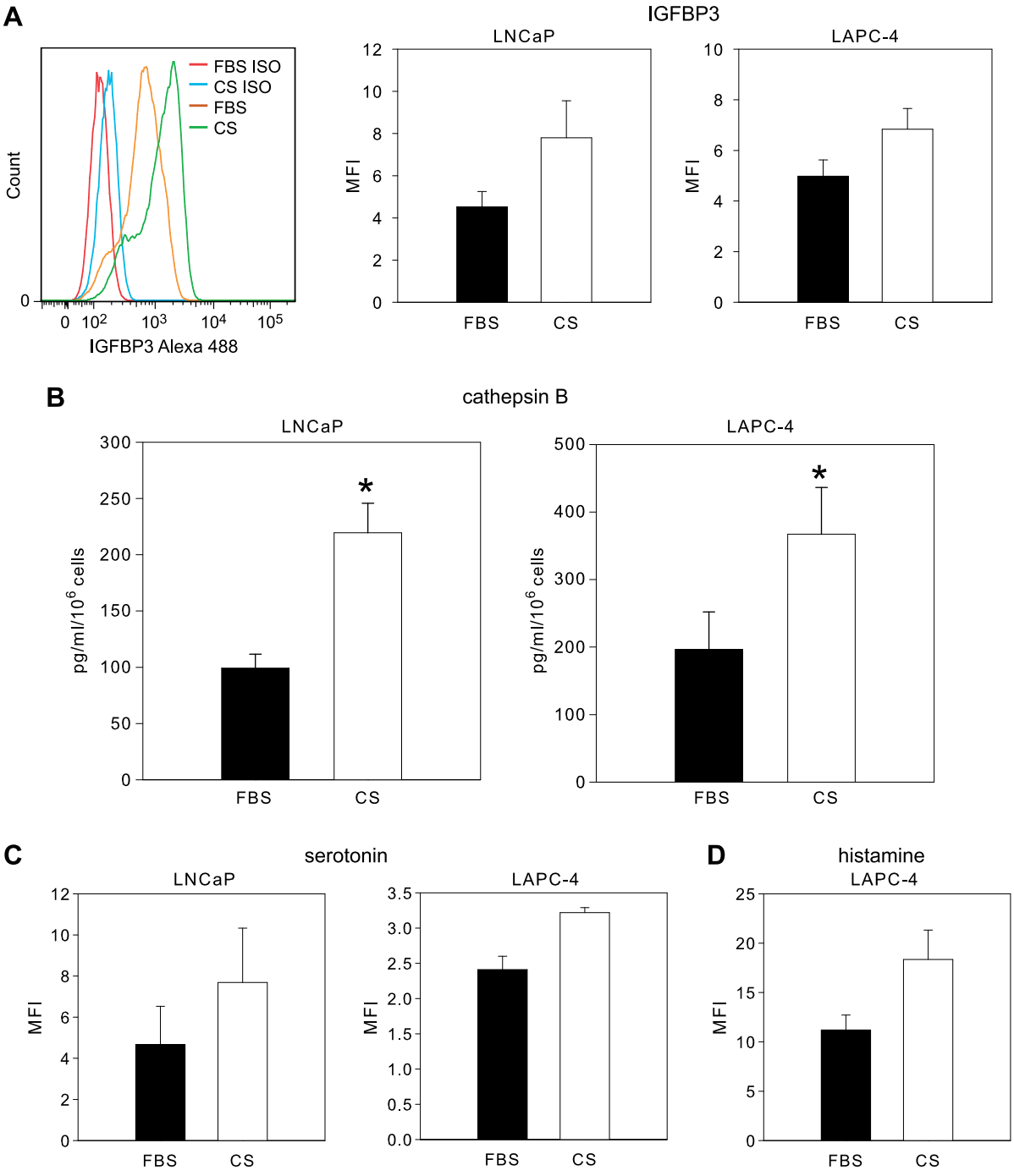

Figure 2. Analysis of markers of the senescent secretome and of NED after androgen depletion. (A) Flow cytometric analysis of IGFBP3 in LNCaP and LAPC-4 cells cultivated for 8 days under the growth conditions indicated (see Materials and Methods). Histogram represents typical result obtained by flow cytometric analysis. Error bars, MFI ± SD from two independent experiments. (B) Cathepsin B concentration, determined by ELISA, in medium conditioned by LNCaP or LAPC-4 cells cultivated for 8 days with or without androgen. Error bars, mean ± SD from four experiments. *Statistical significance ($P < .05$). (C) Flow cytometric analysis of serotonin in LNCaP and LAPC-4 cells and (D) histamine in LAPC-4 cells cultivated for 8 days with or without androgen. Error bars, MFI ± SD from two independent experiments.

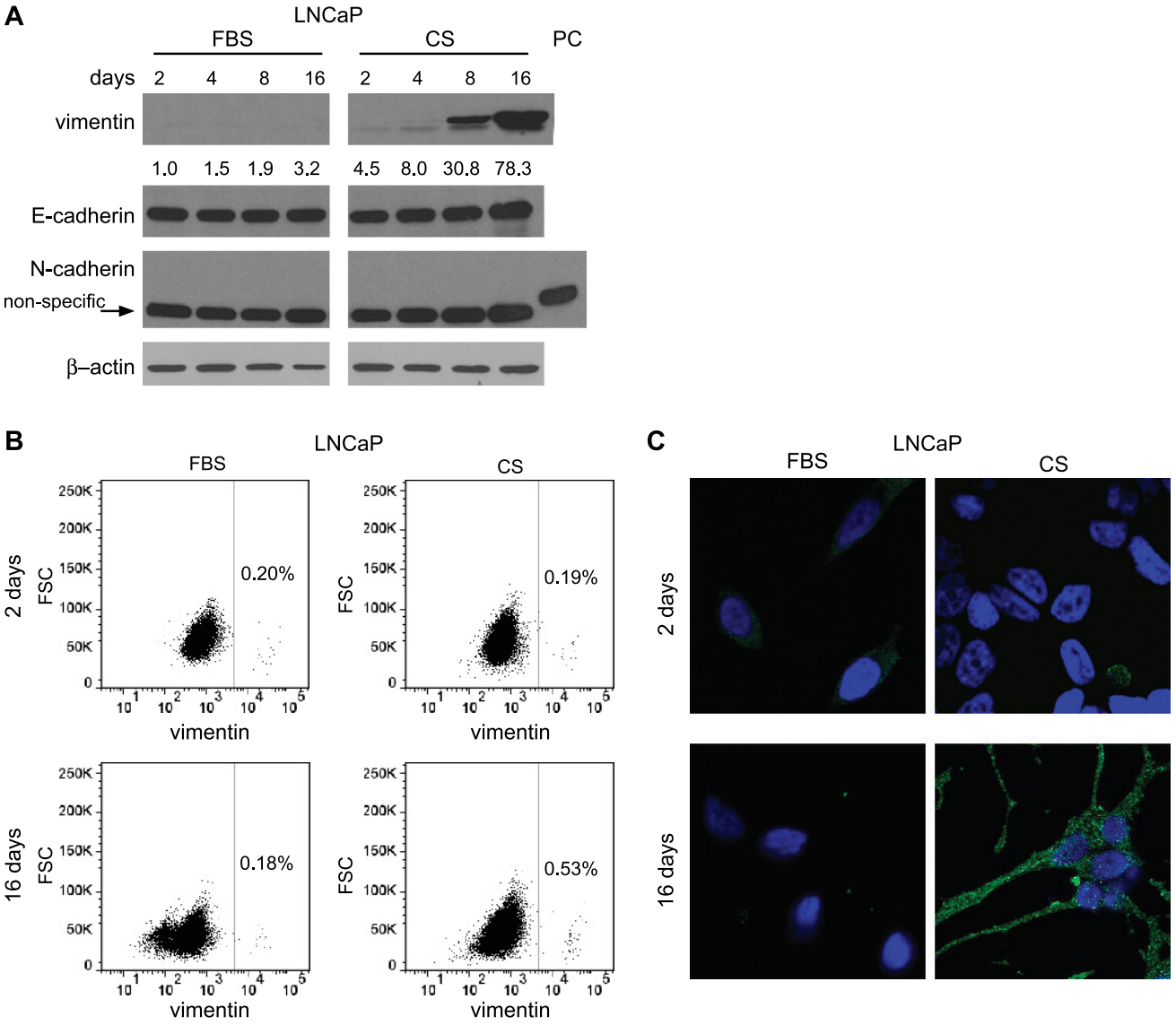

Figure 3. Androgen depletion induces expression of vimentin in LNCaP cells. (A) Western blot analysis of vimentin, E-cadherin, and N-cadherin. (PC, positive control: whole-cell extract from mouse brain.) (B) Flow cytometric analysis showing the percentage of cells expressing high levels of vimentin. Similar results were obtained from three independent experiments. (C) Immunocytochemical detection of vimentin in cultured cells.

In contrast, LNCaP cells grown in CS medium remained senescent and nonproliferative even after reseeding at a low density and cultivating in the presence of androgens (Figure W2, *A-C*, 16D CS + FBS). Induction of NED after androgen depletion was also irreversible (data not shown).

In summary, these data show that long-term androgen depletion in our *in vitro* model induced irreversible senescence and that this was associated with increased expression of senescence-associated secretory factors and markers of NED.

Androgen Depletion Induces Vimentin Expression in Prostate Cancer Cells

To further investigate the phenotype of prostate cancer cells undergoing senescence and NED in response to androgen depletion, we analyzed the expression of cytokeratin and vimentin, which are markers of epithelial cells and mesenchymal cells, respectively. Using a pan-cytokeratin antibody, we found that androgen depletion, as well as high cell density, upregulated the expression of several cytokeratins (Figure W3). We also found that vimentin was strongly induced by androgen depletion (Figure 3*A*). Induction of a strongly positive vimentin subpopulation was confirmed using flow cytometry (Figure 3*B*) and confocal microscopy (Figure 3*C*). Vimentin expression in epithelial cells may indicate an epithelial-to-mesenchymal transition (EMT) [37]. To examine whether EMT occurred in our cultures, we examined the expression of N-cadherin and E-cadherin, which are upregulated and downregulated, respectively, during EMT [38]. N-cadherin was not expressed by LNCaP cells either before or after androgen depletion, and the expression of the epithelial marker E-cadherin was not significantly downregulated after androgen withdrawal (Figure 3*A*). These data indicate that the up-regulation of vimentin after androgen depletion is unlikely to be due to EMT. Because vimentin is also expressed in senescent fibroblasts [39], it is possible that induction of vimentin in our model is indicative of senescence.

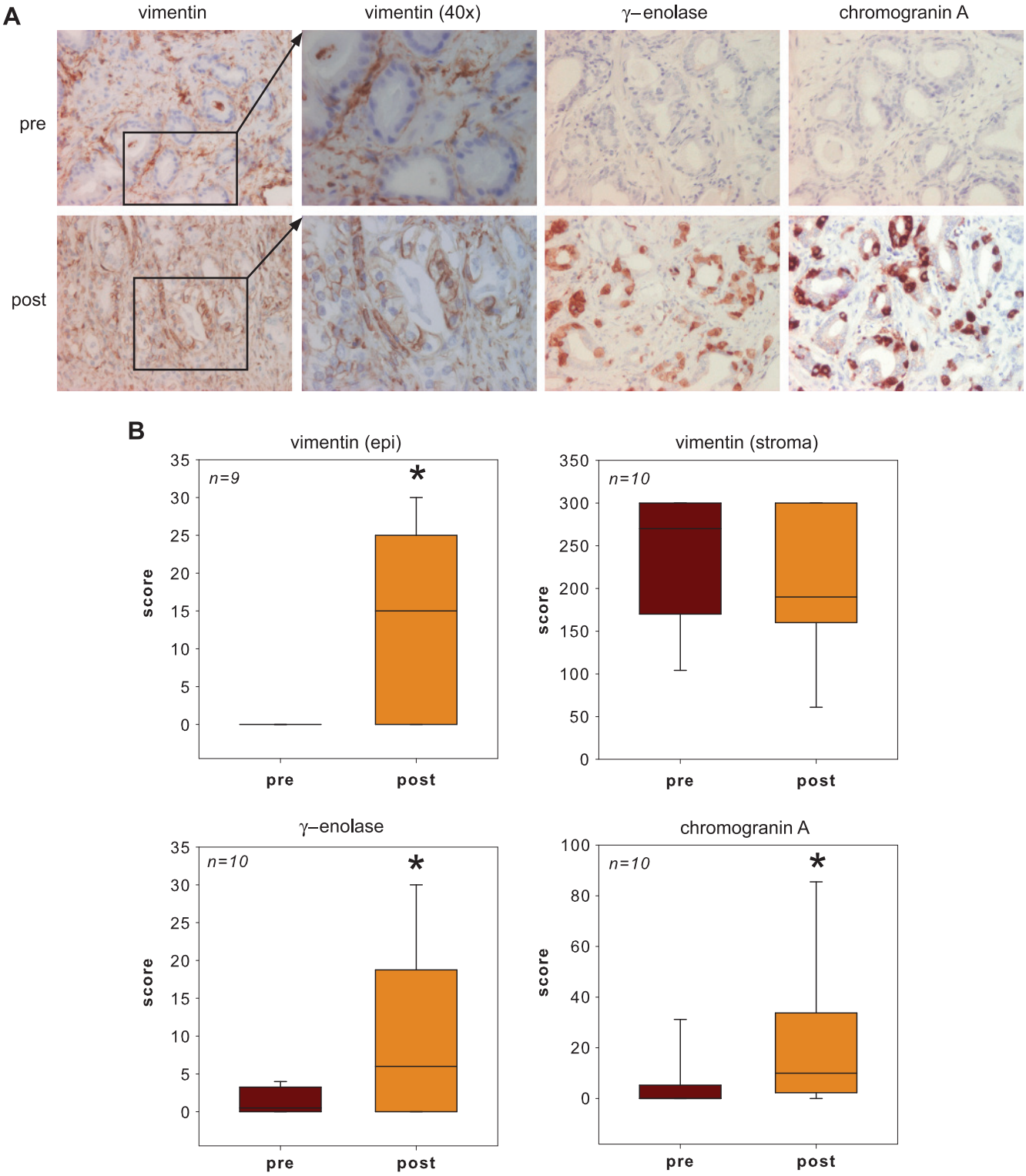

Figure 4. Up-regulation of vimentin and NED markers in human prostate cancer epithelial cells after neoadjuvant ADT. (A) Immunohistochemical detection of γ-enolase, chromogranin A, and vimentin. Sample pairs are from the same individual preneoadjuvant and postneoadjuvant ADT. Expression of vimentin in epithelial and stromal cells is easily distinguishable at 40× magnification (inset). (B) Quantification of γ-enolase, chromogranin A, and vimentin expression in patient tumor samples. *Statistical significance ($P < .05$) compared with samples from patients before receiving ADT.

We wanted to know if induction of vimentin occurred in human prostate tumors after ADT and examined expression of vimentin, as well as the NED markers chromogranin A and γ-enolase, in samples of human prostate cancers collected pre- and/or postneoadjuvant ADT (Table W1). Before ADT, the expression of vimentin, chromogranin A, and γ-enolase in epithelial cells of the prostate tumor samples was either undetectable or at low levels (Figure 4, *A* and *B*, *pre*, *epi*). After ADT, the expression of all three markers was significantly increased in epithelial

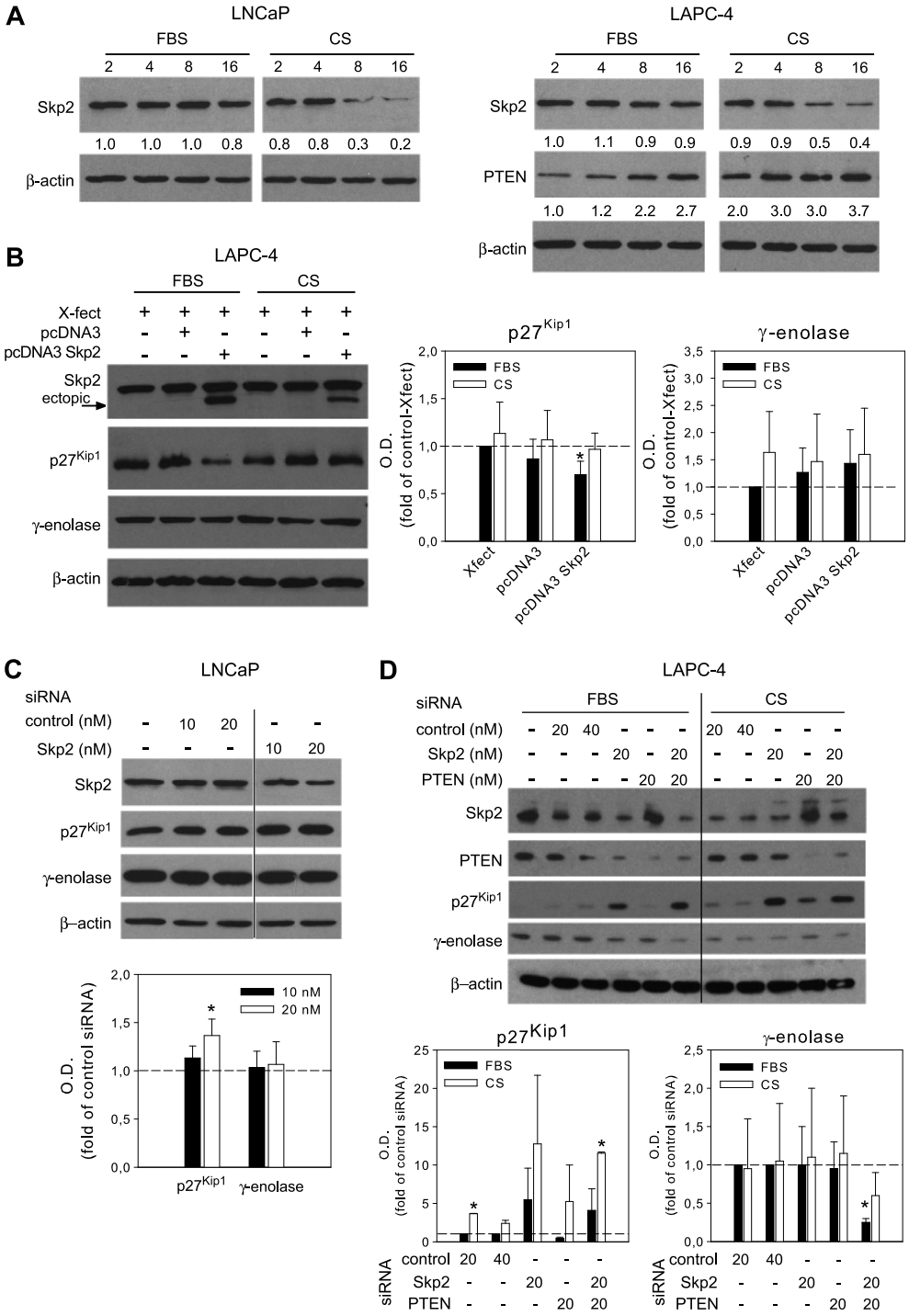

Figure 5. Down-regulation of Skp2 by androgen depletion induced senescence in prostate cancer cells. (A) Western blot detection of Skp2 and PTEN expression in cells cultivated in the presence (FBS) or absence (CS) of androgens. (B) Western blot analysis of Skp2, $p27^{Kip1}$, and γ-enolase after overexpression of Skp2 in LAPC-4 cells. (C) Western blot analysis of Skp2, $p27^{Kip1}$, and γ-enolase in LNCaP cells transfected with control or Skp2-specific siRNA followed by incubation in FBS. (D) Western blot analysis of Skp2, $p27^{Kip1}$, PTEN, and γ-enolase in LAPC-4 cells transfected with control, Skp2-, or PTEN-specific siRNA followed by incubation in presence (FBS) or absence (CS) of androgens for 48 hours. The bar graphs represent the average optical density (OD) ± SD. (E) Frequency of SA-β-gal–positive cells after transfection with control or Skp2 specific siRNA followed by cultivation for 48 hours in the presence (FBS) or absence (CS) of androgens. A minimum of 1000 cells was counted for each experimental group. *Statistical significance ($P < .05$) compared with the cells cultivated in FBS. #Statistical significance ($P < .05$) compared with cells cultivated for 2 days in CS.

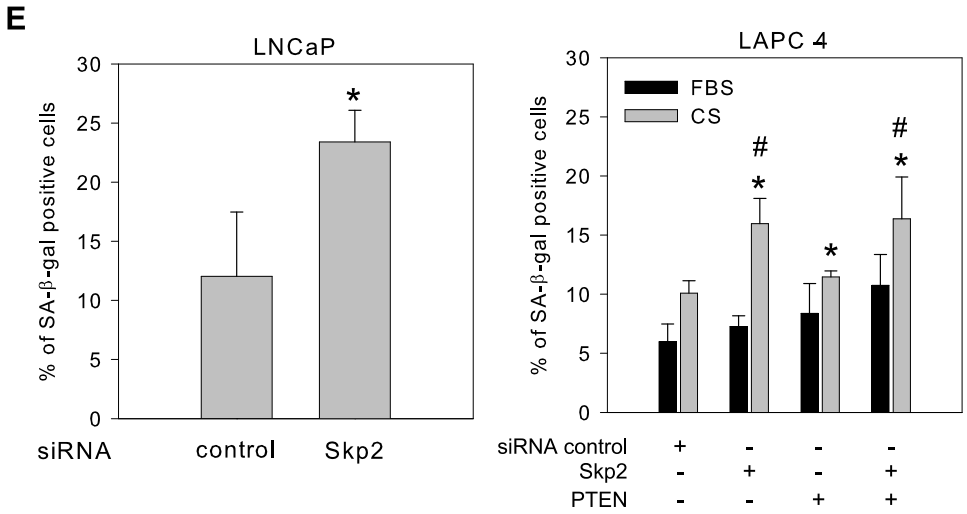

Figure 5. (*continued*).

cells in samples from the same individuals (Figure 4*A*, *post*), and their scores were significantly higher (Figure 4*B*). In contrast, vimentin expression in stromal cells of the prostate was unaffected by ADT. These results show that induction of senescence and NED is associated with the expression of vimentin in epithelial prostate cancer cells.

Role of PTEN-Skp2 Signaling in the Induction of Senescence by Androgen Depletion

PTEN-Skp2 signaling is a crucial regulator of $p27^{Kip1}$ and senescence [15,26,27]. In LNCaP and LAPC-4 cells grown without androgens, Skp2 became downregulated, whereas the level of PTEN increased over time (Figure 5*A*). LNCaP cells were PTEN null [33] and were not assayed for PTEN. Because Skp2 expression can be controlled by AR, and androgen depletion led to up-regulation of $p27^{Kip1}$ in our model (data not shown), we examined the role of PTEN and Skp2 in androgen depletion–induced NED and senescence. Transient transfection of LAPC-4 cells with the Skp2 expression vector [40] led to a slight decrease in $p27^{Kip1}$ expression (Figure 5*B*), whereas partial depletion of Skp2 using RNA interference was sufficient to upregulate $p27^{Kip1}$ in both LNCaP and LAPC-4 cells (Figure 5, *C* and *D*). Interestingly, although depletion of Skp2 alone had no effect on the level of γ-enolase, codepletion of Skp2 and PTEN with siRNA did cause γ-enolase to decrease in LAPC-4 cells grown under normal or androgen-depleted conditions (Figure 5*D*). Finally, down-regulation of Skp2 by transfection with Skp2 siRNA was followed by a significant increase in the number of SA-β-gal–positive cells in LNCaP cultures grown in the presence of androgens, as well as in LAPC-4 cultures grown without androgens (Figure 5*E*). These data show that down-regulation of Skp2 by androgen depletion contributes to the induction of senescence in prostate cancer cells and that Skp2 is not involved in NED.

Discussion

To our knowledge, this is the first demonstration that androgen depletion induces senescence of prostate cancer cells paralleled with up-regulation of vimentin expression. Senescence, a permanent cell cycle arrest coupled with resistance to apoptosis and high metabolic activity, is a potent defense against tumorigenesis. However, it is now becoming clear that cells with a SASP may actually promote tumor progression through their secretion of factors that can significantly modulate the tissue microenvironment [21,41,42]. Using a panel of markers to identify senescent cells, including SA-β-gal activity, telomerase activity, and formation of HP1β foci, we have found that androgen depletion induced irreversible senescence in prostate cancer cells *in vitro*. We also found that expression of both cathepsin B and IGFBP3, two markers of SASP [11,43], was significantly increased after androgen depletion and confirmed that androgen depletion promoted NED of prostate cancer cells [44]. This is the first demonstration that androgen depletion leads to senescence and NED of prostate cancer cells. Interestingly, senescent and NE-like cells are associated with high metabolic activity and the potential to influence the behavior of nonsenescent neighboring cells.

To further characterize the phenotype of prostate cancer cells after androgen depletion, we examined markers of epithelial and mesenchymal cells. Surprisingly, ADT increased the expression of the epithelial marker cytokeratin and the mesenchymal marker vimentin [45]. Similar findings were observed in tumor samples from prostate cancer patients after ADT, and these are the first demonstration that androgen depletion upregulates vimentin in prostate cancer epithelial cells. Moreover, vimentin expression was paralleled with the expression of NED markers γ-enolase and chromogranin A. Although vimentin is a well-known marker of EMT [37], it is also expressed by senescent fibroblasts [39]. Because the expression of both N-cadherin and E-cadherin was unaffected by androgen depletion, the NE-like cells in our cultures were unlikely to be undergoing an EMT [38]. Instead, the robust expression of vimentin after androgen depletion may be associated with the induction of senescence in prostate cancer epithelial cells.

Skp2 was recently implicated in promoting oncogene-induced senescence [26]. In the prostate, as well as in our system, inhibition of AR is correlated with down-regulation of Skp2 and decreased proliferation [30,31]. We addressed the causal relationship between these findings and found that depletion of Skp2 using RNAi was sufficient to induce senescence in LNCaP cells and also significantly potentiated androgen depletion-induced senescence in LAPC-4 cells. These results indicate that down-regulation of Skp2 is an important component of the mechanism through which androgen depletion induces senescence in prostate cancer cells. Although down-regulation of Skp2 was recently reported to induce senescence in the context of PTEN inactivation [26],

our data clearly demonstrate that Skp2 inactivation is sufficient to promote senescence even in the presence of elevated levels of PTEN. Presumably another mechanism, perhaps loss of heterozygosity of TP53, is involved in Skp2-mediated induction of senescence in LAPC-4 cells [46].

Our findings demonstrate a novel linkage between the inhibition of AR activity, down-regulation of Skp2, and the formation of secretory, senescent cells in prostate tumors. These observations suggest that modulation of the prostate tumor microenvironment after androgen depletion is a major contributory factor in the development of androgen-independent prostatic cancer, especially because several components of the SASP secretome (e.g., IL-6, IL-8, KGH, and epidermal growth factor) are capable of transactivating AR under androgen-depleted conditions [7–9]. We speculate that, in prostate cancer patients undergoing ADT, paracrine factors released by senescent cells override the requirement for androgen ligand and promote the clonal expansion of androgen-independent cells, leading to failure of ADT and progression of the disease to androgen independence.

Acknowledgments

The authors thank K. Nakayama for his kind gift of the Skp2 expression plasmid; Dr Robert Reiter for his kind gift of LAPC-4 cells; Dr Eva Bártová for her help with HP1β detection; and Iva Lišková, Hana Finsterlová, Jaromíra Netíková, Eva Sedláková, and Kateřina Svobodová for their superb technical assistance.

References

[1] Harris WP, Mostaghel EA, Nelson PS, and Montgomery B (2009). Androgen deprivation therapy: progress in understanding mechanisms of resistance and optimizing androgen depletion. *Nat Clin Pract Urol* **6**, 76–85.

[2] Sharifi N, Gulley JL, and Dahut WL (2010). An update on androgen deprivation therapy for prostate cancer. *Endocr Relat Cancer* **17**, R305–R315.

[3] De La Taille A, Vacherot F, Salomon L, Druel C, Gil Diez De Medina S, Abbou C, Buttyan R, and Chopin D (2001). Hormone-refractory prostate cancer: a multistep and multi-event process. *Prostate Cancer Prostatic Dis* **4**, 204–212.

[4] Nelson EC, Cambio AJ, Yang JC, Ok JH, Lara PN Jr, and Evans CP (2007). Clinical implications of neuroendocrine differentiation in prostate cancer. *Prostate Cancer Prostatic Dis* **10**, 6–14.

[5] Sun Y, Niu J, and Huang J (2009). Neuroendocrine differentiation in prostate cancer. *Am J Transl Res* **1**, 148–162.

[6] Nelson WG, De Marzo AM, and Isaacs WB (2003). Prostate cancer. *N Engl J Med* **349**, 366–381.

[7] Culig Z, Hobisch A, Cronauer MV, Radmayr C, Trapman J, Hittmair A, Bartsch G, and Klocker H (1994). Androgen receptor activation in prostatic tumor cell lines by insulin-like growth factor-I, keratinocyte growth factor, and epidermal growth factor. *Cancer Res* **54**, 5474–5478.

[8] Malinowska K, Neuwirt H, Cavarretta IT, Bektic J, Steiner H, Dietrich H, Moser PL, Fuchs D, Hobisch A, and Culig Z (2009). Interleukin-6 stimulation of growth of prostate cancer *in vitro* and *in vivo* through activation of the androgen receptor. *Endocr Relat Cancer* **16**, 155–169.

[9] Seaton A, Scullin P, Maxwell PJ, Wilson C, Pettigrew J, Gallagher R, O'Sullivan JM, Johnston PG, and Waugh DJ (2008). Interleukin-8 signaling promotes androgen-independent proliferation of prostate cancer cells via induction of androgen receptor expression and activation. *Carcinogenesis* **29**, 1148–1156.

[10] Feldman BJ and Feldman D (2001). The development of androgen-independent prostate cancer. *Nat Rev Cancer* **1**, 34–45.

[11] Coppe JP, Desprez PY, Krtolica A, and Campisi J (2010). The senescence-associated secretory phenotype: the dark side of tumor suppression. *Annu Rev Pathol* **5**, 99–118.

[12] Campisi J and d'Adda di Fagagna F (2007). Cellular senescence: when bad things happen to good cells. *Nat Rev Mol Cell Biol* **8**, 729–740.

[13] Serrano M, Lin AW, McCurrach ME, Beach D, and Lowe SW (1997). Oncogenic *ras* provokes premature cell senescence associated with accumulation of p53 and $p16^{INK4a}$. *Cell* **88**, 593–602.

[14] Bartkova J, Rezaei N, Liontos M, Karakaidos P, Kletsas D, Issaeva N, Vassiliou LV, Kolettas E, Niforou K, Zoumpourlis VC, et al. (2006). Oncogene-induced senescence is part of the tumorigenesis barrier imposed by DNA damage checkpoints. *Nature* **444**, 633–637.

[15] Chen Z, Trotman LC, Shaffer D, Lin HK, Dotan ZA, Niki M, Koutcher JA, Scher HI, Ludwig T, Gerald W, et al. (2005). Crucial role of p53-dependent cellular senescence in suppression of Pten-deficient tumorigenesis. *Nature* **436**, 725–730.

[16] Alimonti A, Nardella C, Chen Z, Clohessy JG, Carracedo A, Trotman LC, Cheng K, Varmeh S, Kozma SC, Thomas G, et al. (2010). A novel type of cellular senescence that can be enhanced in mouse models and human tumor xenografts to suppress prostate tumorigenesis. *J Clin Invest* **120**, 681–693.

[17] Allsopp RC and Harley CB (1995). Evidence for a critical telomere length in senescent human fibroblasts. *Exp Cell Res* **219**, 130–136.

[18] Chen Q and Ames BN (1994). Senescence-like growth arrest induced by hydrogen peroxide in human diploid fibroblast F65 cells. *Proc Natl Acad Sci USA* **91**, 4130–4134.

[19] Ewald J, Desotelle J, Almassi N, and Jarrard D (2008). Drug-induced senescence bystander proliferation in prostate cancer cells *in vitro* and *in vivo*. *Br J Cancer* **98**, 1244–1249.

[20] Elmore LW, Rehder CW, Di X, McChesney PA, Jackson-Cook CK, Gewirtz DA, and Holt SE (2002). Adriamycin-induced senescence in breast tumor cells involves functional p53 and telomere dysfunction. *J Biol Chem* **277**, 35509–35515.

[21] Krtolica A, Parrinello S, Lockett S, Desprez PY, and Campisi J (2001). Senescent fibroblasts promote epithelial cell growth and tumorigenesis: a link between cancer and aging. *Proc Natl Acad Sci USA* **98**, 12072–12077.

[22] Lawrenson K, Grun B, Benjamin E, Jacobs IJ, Dafou D, and Gayther SA (2010). Senescent fibroblasts promote neoplastic transformation of partially transformed ovarian epithelial cells in a three-dimensional model of early stage ovarian cancer. *Neoplasia* **12**, 317–325.

[23] Dean JP and Nelson PS (2008). Profiling influences of senescent and aged fibroblasts on prostate carcinogenesis. *Br J Cancer* **98**, 245–249.

[24] Coppe JP, Patil CK, Rodier F, Sun Y, Munoz DP, Goldstein J, Nelson PS, Desprez PY, and Campisi J (2008). Senescence-associated secretory phenotypes reveal cell-nonautonomous functions of oncogenic RAS and the p53 tumor suppressor. *PLoS Biol* **6**, 2853–2868.

[25] Caino MC, Meshki J, and Kazanietz MG (2009). Hallmarks for senescence in carcinogenesis: novel signaling players. *Apoptosis* **14**, 392–408.

[26] Lin HK, Chen Z, Wang G, Nardella C, Lee SW, Chan CH, Yang WL, Wang J, Egia A, Nakayama KI, et al. (2010). Skp2 targeting suppresses tumorigenesis by Arf-p53–independent cellular senescence. *Nature* **464**, 374–379.

[27] Nakayama KI and Nakayama K (2005). Regulation of the cell cycle by SCF-type ubiquitin ligases. *Semin Cell Dev Biol* **16**, 323–333.

[28] Yang G, Ayala G, De Marzo A, Tian W, Frolov A, Wheeler TM, Thompson TC, and Harper JW (2002). Elevated Skp2 protein expression in human prostate cancer: association with loss of the cyclin-dependent kinase inhibitor p27 and PTEN and with reduced recurrence-free survival. *Clin Cancer Res* **8**, 3419–3426.

[29] Ben-Izhak O, Lahav-Baratz S, Meretyk S, Ben-Eliezer S, Sabo E, Dirnfeld M, Cohen S, and Ciechanover A (2003). Inverse relationship between Skp2 ubiquitin ligase and the cyclin dependent kinase inhibitor $p27^{Kip1}$ in prostate cancer. *J Urol* **170**, 241–245.

[30] Wang H, Sun D, Ji P, Mohler J, and Zhu L (2008). An AR-Skp2 pathway for proliferation of androgen-dependent prostate-cancer cells. *J Cell Sci* **121**, 2578–2587.

[31] Lu L, Schulz H, and Wolf DA (2002). The F-box protein SKP2 mediates androgen control of p27 stability in LNCaP human prostate cancer cells. *BMC Cell Biol* **3**, 22.

[32] Klein KA, Reiter RE, Redula J, Moradi H, Zhu XL, Brothman AR, Lamb DJ, Marcelli M, Belldegrun A, Witte ON, et al. (1997). Progression of metastatic human prostate cancer to androgen independence in immunodeficient SCID mice. *Nat Med* **3**, 402–408.

[33] Lincova E, Hampl A, Pernicova Z, Starsichova A, Krcmar P, Machala M, Kozubik A, and Soucek K (2009). Multiple defects in negative regulation of the PKB/Akt pathway sensitise human cancer cells to the antiproliferative effect of non-steroidal anti-inflammatory drugs. *Biochem Pharmacol* **78**, 561–572.

[34] Dimri GP, Lee X, Basile G, Acosta M, Scott G, Roskelley C, Medrano EE, Linskens M, Rubelj I, Pereira-Smith O, et al. (1995). A biomarker that identifies senescent human cells in culture and in aging skin *in vivo*. *Proc Natl Acad Sci USA* **92**, 9363–9367.

[35] Gary RK and Kindell SM (2005). Quantitative assay of senescence-associated beta-galactosidase activity in mammalian cell extracts. *Anal Biochem* **343**, 329–334.

[36] Shay JW and Wright WE (2005). Senescence and immortalization: role of telomeres and telomerase. *Carcinogenesis* **26**, 867–874.

[37] Zeisberg M (2009). Biomarkers for epithelial-mesenchymal transitions. *J Clin Invest* **119**, 1429–1437.

[38] Lee JM, Dedhar S, Kalluri R, and Thompson EW (2006). The epithelial-mesenchymal transition: new insights in signaling, development, and disease. *J Cell Biol* **172**, 973–981.

[39] Nishio K, Inoue A, Qiao S, Kondo H, and Mimura A (2001). Senescence and cytoskeleton: overproduction of vimentin induces senescent-like morphology in human fibroblasts. *Histochem Cell Biol* **116**, 321–327.

[40] Nakayama K, Nagahama H, Minamishima YA, Matsumoto M, Nakamichi I, Kitagawa K, Shirane M, Tsunematsu R, Tsukiyama T, Ishida N, et al. (2000). Targeted disruption of Skp2 results in accumulation of cyclin E and p27(Kip1), polyploidy and centrosome overduplication. *EMBO J* **19**, 2069–2081.

[41] Sprenger CC, Drivdahl RH, Woodke LB, Eyman D, Reed MJ, Carter WG, and Plymate SR (2008). Senescence-induced alterations of laminin chain expression modulate tumorigenicity of prostate cancer cells. *Neoplasia* **10**, 1350–1361.

[42] Coppe JP, Patil CK, Rodier F, Krtolica A, Beausejour CM, Parrinello S, Hodgson JG, Chin K, Desprez PY, and Campisi J (2010). A human-like senescence-associated secretory phenotype is conserved in mouse cells dependent on physiological oxygen. *PLoS One* **5**, e9188.

[43] Untergasser G, Koch HB, Menssen A, and Hermeking H (2002). Characterization of epithelial senescence by serial analysis of gene expression: identification of genes potentially involved in prostate cancer. *Cancer Res* **62**, 6255–6262.

[44] Yuan TC, Veeramani S, Lin FF, Kondrikou D, Zelivianski S, Igawa T, Karan D, Batra SK, and Lin MF (2006). Androgen deprivation induces human prostate epithelial neuroendocrine differentiation of androgen-sensitive LNCaP cells. *Endocr Relat Cancer* **13**, 151–167.

[45] Kalluri R (2009). EMT: when epithelial cells decide to become mesenchymal-like cells. *J Clin Invest* **119**, 1417–1419.

[46] van Bokhoven A, Varella-Garcia M, Korch C, Johannes WU, Smith EE, Miller HL, Nordeen SK, Miller GJ, and Lucia MS (2003). Molecular characterization of human prostate carcinoma cell lines. *Prostate* **57**, 205–225.

Supplementary Materials and Methods

Induction of Senescence in Human Foreskin Fibroblast Cell Line HFF-1 with Hydrogen Peroxide

Human foreskin fibroblast HFF-1 cells (ATCC, LGC Standards Sp. z.o.o., Lomianki, Poland) were cultivated in DMEM (Sigma) supplemented with 15% FBS. Senescence was induced in HFF-1 cells as described previously [1]. Cells were seeded at a density of 25,000/cm^2 in complete media. After 24 hours, the medium was replaced, the cells were treated with 200 μM H_2O_2 for 2 hours, and the medium was replaced by fresh medium without H_2O_2. Treated cells were cultivated for another 96 hours with one change of growth medium. After 96 hours, the cells were reseeded at a density of 25,000/cm^2 and allowed to recover for 24 hours before the second treatment with 200 μM H_2O_2. Treated cells were cultivated for an additional 6 to 7 days and then harvested for further analysis.

Cell Number Assessment

The cell numbers were determined using a Coulter Counter ZM (Beckman Coulter, Brea, CA).

Experimental Design and Sample Collection for ELISA

For the collection of conditioned medium for ELISA analysis, the cells were cultivated as described in the Materials and Methods for 2 or 8 days. The last medium exchange was performed 48 hours before medium collection. Cellular debris was removed from conditioned medium by centrifugation (500*g*, 10 minutes), and the supernatant was stored at −80°C. Cathepsin B detection was performed according to the manufacturer's recommendation. The absorbance values were normalized to cell number.

Antibodies for Western Blot Analysis

Primary antibodies against human γ-enolase (sc-21738) and PTEN (sc-7974) were obtained from Santa Cruz Biotechnology; cytokeratin (CK) 7 + 17 (11-109-C100), CK 8 (11-104-C100), CK 18 (11-106-C100), and pan-reactive CK (11-108-C100) antibodies were from Exbio, Prague, Czech Republic; $p27^{Kip1}$ (610242), E-cadherin (610182), and N-cadherin (610920) antibodies were from BD Pharmingen, San Jose, CA; vimentin (V6389), β-actin (A5441), and α-tubulin (T9026) antibodies were from Sigma; Skp2 (no. 313) was from Cell Signaling Technology, Danvers, MA; horseradish peroxidase–conjugated antimouse IgG (no. NA931) and antirabbit IgG (no. NA934) were from GE Healthcare, Chalfont St Giles, United Kingdom.

Antibodies for Flow Cytometric Detection

The following primary antibodies were used: vimentin (V6389), serotonin (S5545), histamine (H7403), and IGFBP3 (HPA013357, all from Sigma). Afterward, the cells were washed and incubated with the appropriate secondary antibody conjugated with Alexa Fluor 488 (Invitrogen). Far red LIVE/DEAD Fixable Dead Cell Stain Kit (Invitrogen) was used for the exclusion of dead cells.

Antibodies for Immunofluorescence and Confocal Microscopy

For the detection of HP1β (07-333; Upstate), phospho-H2AX (Ser 139, 05-636; Upstate, Millipore, Billerica, MA) and vimentin (V6389), the cells were fixed with 4% paraformaldehyde, permeabilized with 0.1% Triton X-100 and 0.1% saponin, blocked with 1% bovine serum albumin, washed, and incubated with primary antibody overnight at 4°C [2]. The samples were then incubated with the appropriate secondary antibody conjugated with Alexa Fluor 488 or Alexa Fluor 594 (Invitrogen).

Antibodies for Immunocytochemistry

The following antibodies were used: γ-enolase (anti-NSE, clone BBS/NC/VI-H14; Serotec, Kidlington, United Kingdom), vimentin (V9; Dako, Glostrup, Denmark), chromogranin A antibody (LK2H10; Serotec), and secondary antibody (Dual Link; Dako).

Supplementary References

[1] Chen J-H, Ozanne SE, and Hales CN (2007). Methods of cellular senescence induction using oxidative stress. In *Methods in Molecular Biology: Biological Aging: Methods and Protocols*. TO Tollefsbol (Ed). Humana Press, Inc, Totowa, NJ. pp. 179–190.

[2] Bartova E, Galiova G, Krejci J, Harnicarova A, Strasak L, and Kozubek S (2008). Epigenome and chromatin structure in human embryonic stem cells undergoing differentiation. *Dev Dyn* **237**, 3690–3702.

Table W1. Characteristics of Human Prostate Tumor Samples.

Patient No.	Age at dg (yr)	PSA at dg	Neoadjuvant Therapy	Tissue	pT	pN	GS
1	55	83.5	HFM	Both	pT3b	pN0	5 + 3
2	68	108.4	BIC	Both	pT3b	pN1	3 + 4
3	54	60	HFM, LHRH	Both	pT4	pN0	3 + 3
4	60	9.7	BIC, HFM, LHRH	Both	pT2b	pN0	3 + 4
5	64	52	HFM	After	pT3a	pN1	4 + 5
6	58	29.1	HFM	After	pT2b	pN0	3 + 4
7	50	47.2	HFM	After	pT3b	pN1	4 + 5
8	54	24.39	HFM, CPA	After	pT3b	pN0	4 + 5
9	66	8.2	HFM	After	pT2b	pN0	3 + 5
10	63	5.7	BIC, HFM	After	pT2b	pN0	3 + 4
11	59	8.5	None	Before	pT2b	pNx	3 + 4
12	66	7.07	None	Before	pT2b	pN0	4 + 4
13	69	8.22	None	Before	pT3a	pN0	2 + 2
14	63	9.8	None	Before	pT2c	pNx	3 + 4
15	66	32	None	Before	pT2b	pN0	3 + 2
16	66	8.29	None	Before	pT2b	pN0	4 + 5

BIC indicates bicalutamide; CPA, cyproterone acetate; dg, diagnosis; GS, Gleason score; HFM, hydroxyflutamide; LHRH, luteinizing hormone-releasing hormone analog; pNx, no lymphadenectomy; pT, pathologic T stage; Tissue, type of tissue available with respect to the neoadjuvant therapy (before, after, both).

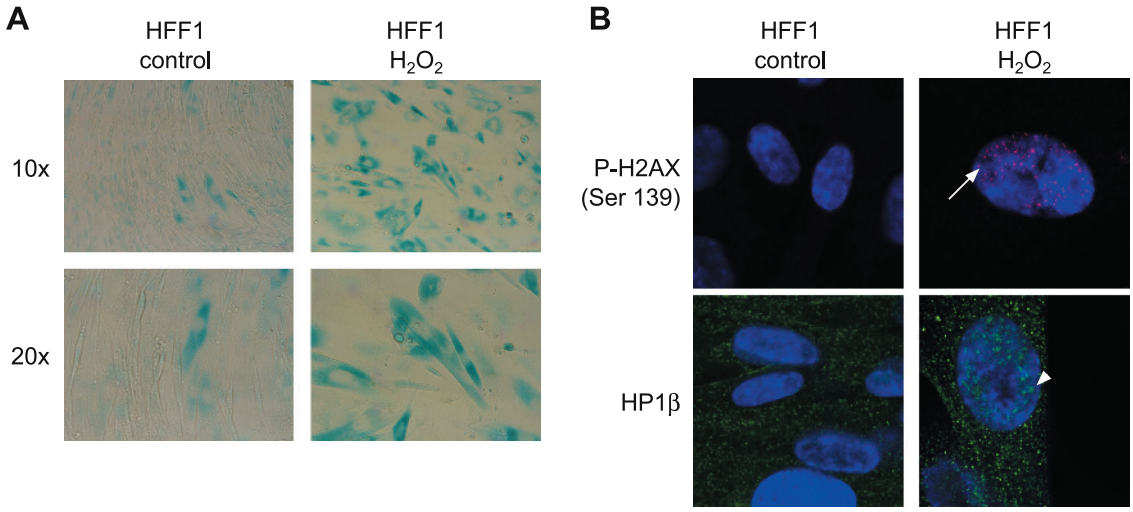

Figure W1. Expression of markers of senescence in human foreskin fibroblasts (HFF-1) cells after exposure to 200 μM hydrogen peroxide (H_2O_2). (A) SA-β-gal staining of control and H_2O_2-treated HFF-1 cells. (B) Confocal images of P-H2AX (S139) and HP1β immunofluorescence in control and H_2O_2-treated HFF-1 cells. White arrow and arrowhead, positive signal for P-H2AX (S139) staining and formation of HP1β foci, respectively.

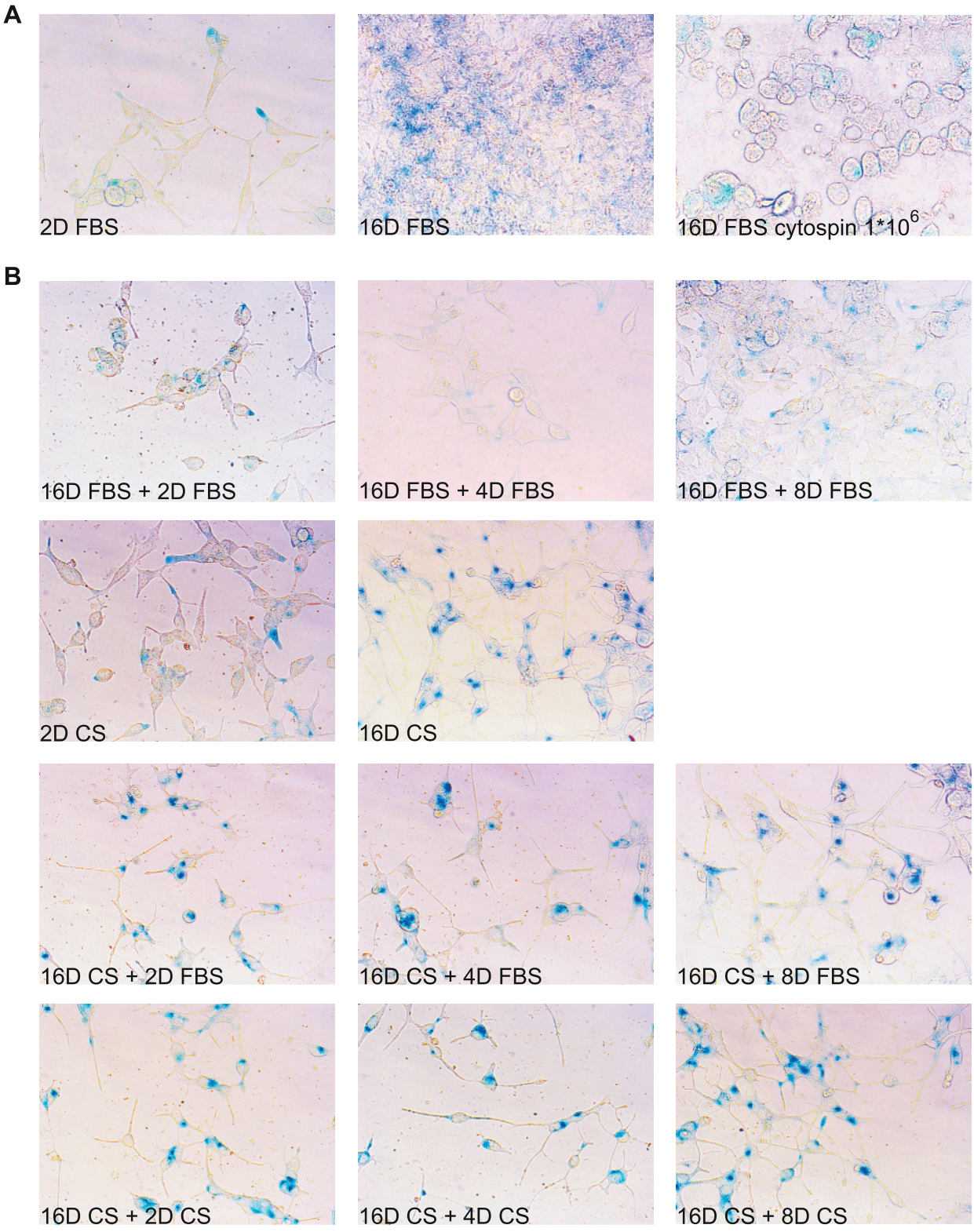

Figure W2. Senescence induced by androgen depletion is irreversible. (A) Cytochemical detection of SA-β-gal activity in long-term cultivated LNCaP cells after reseeding. Cytochemical analysis of SA-β-gal activity showed false positivity in the case of highly confluent cells, when such cells were negative after their dissociation followed by cytospin. (B) The cells were cultivated for 16 days and then reseeded at a low density (10,000 cells/cm^2) in appropriate media. The cells grown in FBS were reseeded in medium with FBS; cells grown in CS were reseeded in medium containing either CS or FBS. Reseeded cells were grown for an additional 2, 4, and 8 days (16 + 2, 16 + 4, and 16 + 8, respectively) without reseeding. (C) Analysis of cell numbers in response to reseeding. Data represent mean ± SD of two independent experiments.

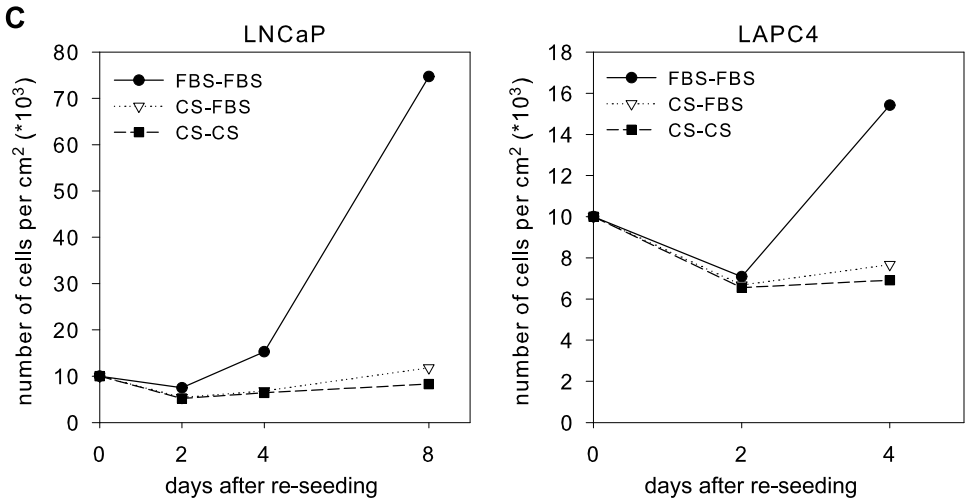

Figure W2. (*continued*).

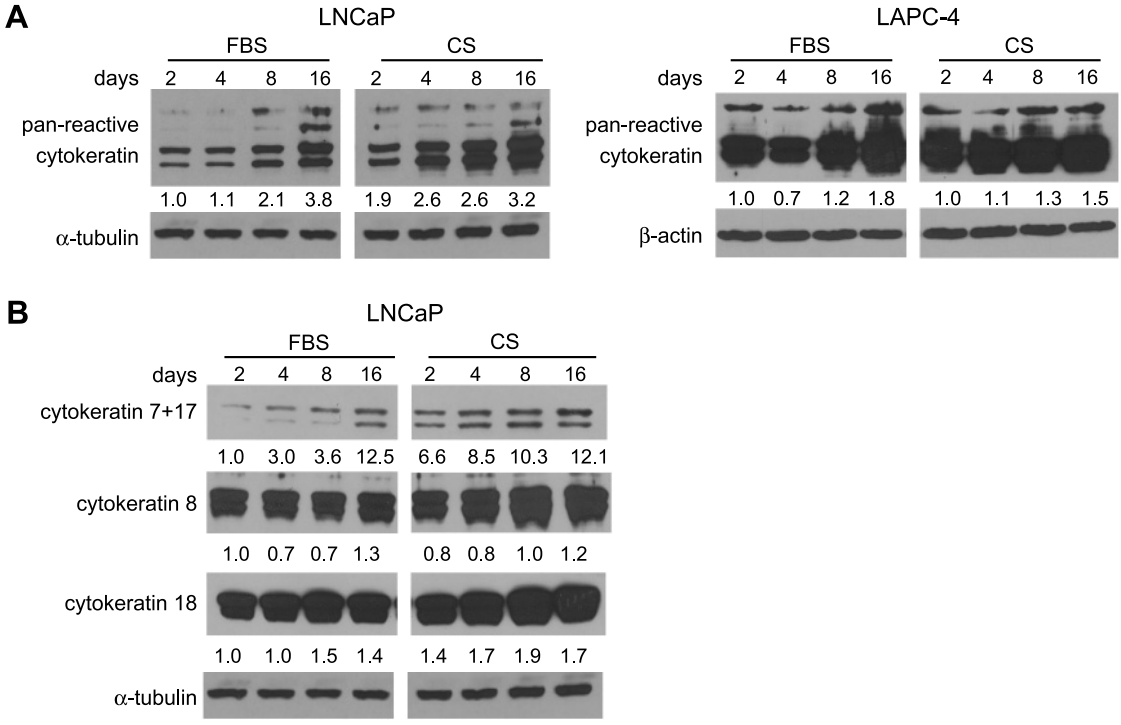

Figure W3. Western blot analysis of expression of cytokeratins in LNCaP and LAPC-4 cells cultivated in the presence (FBS) or absence (CS) of androgens. (A) Expression of cytokeratins detected by a pan-reactive cytokeratin antibody. (B) Cytokeratin 7 + 17, cytokeratin 8, and cytokeratin 18 expression in LNCaP cells. α-Tubulin was used as a loading control.